

Tautomeric Equilibria Revisited: proton-tautomerism in solvent and the fundamentals of molecular stability prediction

A. R. Carvalho^{*,†,‡}

[†]*Available for postdoctoral position*

[‡]*Current address: Niterói, Brazil*

ORCID: 0000-0001-9756-9225

E-mail: andre_carvalho@id.uff.br

Abstract

Understanding the molecular stability is important for predicting the relative reactivity of chemical agents and the relative yields of desirable products. However, over decades, a consistent estimate of a particular chemical equilibrium (proton-tautomerism) has proven challenging. We revisit the molecular orbital analysis in the classic tautomeric oxo-hydroxy case, i.e., 2-pyridone/2-hydroxypyridine in gas-phase and solution, (Wong et al. 1992). Our results indicate the possibility of tuning the tautomeric equilibrium through directing groups. Our findings also reveal the lack of reproducibility of orbital energies as responsible for the remarkable contrast between the results of the wavefunction and density functional methods. Our proposal leads the correction in the estimation of relative stability in excellent agreement with experiments in gas-phase and solution. The analogous approach for different compounds corroborates the reliability of our description on the molecular stability and its potential application, e.g., a guide to estimate the relative stability of molecules, to measure the confidence

of the proposed reaction mechanisms by different theoretical methods, development of the molecular switches and computer-aided drug design.

1 Introduction

Tautomerism is the dynamic equilibrium between molecules with the same atomic composition, where there are a potential barrier and relative energy small enough to allow interconversion.^{1,2} Research on tautomerism covers scientific fields ranging from chemistry, biochemistry to chemical physics. These studies are of fundamental importance in the interpretation of reaction mechanisms involving tautomers,¹ e.g., to stabilize covalent organic frameworks,³ in computer-aided drug design and their biological effects,^{4,5} as a possible factor of spontaneous mutagenesis due to the tautomeric forms of nucleic acid bases^{6,7} and as molecular switches for logic gates, diodes and transistors.^{8,9}

The 2-pyridone/2-hydroxypyridine (2-PY/2-HY) isomerization, see Figure (1), is one of the simplest prototype systems for proton-transfer tautomerism and hydrogen bonding studies, and yet an important heteroaromatic system: Analogous to hydrogen-bonded DNA base pairs,¹⁰ as a design element to catalysis¹¹ with a potential for self-assembly platform of bidentate ligands,¹² an emergent antitumor antiviral agent and building blocks in synthesis.¹³

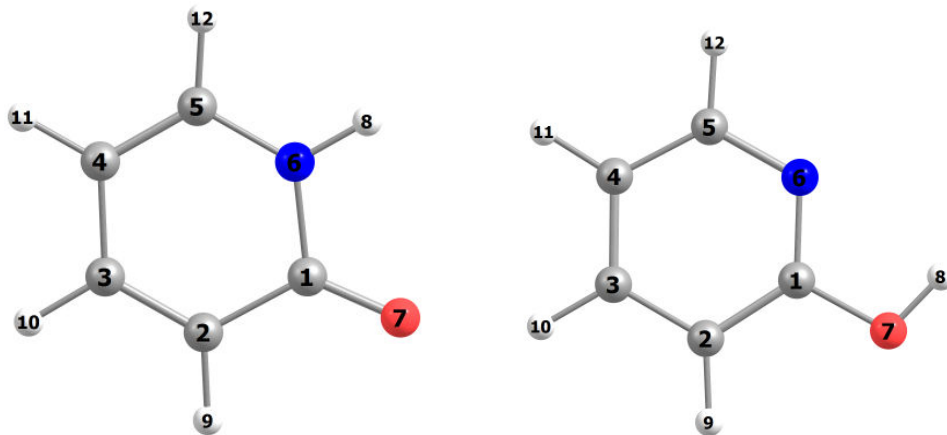


Figure 1: 2-pyridone (left) and 2-hydroxypyridine (right): Molecular structures of the prototypical model for heteroaromatic proton-transfer tautomerism. Molecular formula: C_5H_5NO .

The relative stability on 2-PY/2-HY tautomerism is a focus of investigation for more than a century.^{14,15} Experimental studies include ultraviolet (UV),¹⁶ infrared,^{16,17} photoemission (PES)^{18,19} spectroscopies, to rotationally resolved laser induced fluorescence,²⁰ microwave²¹ spectroscopies and ion cyclotron resonance.²² The measurements of this keto-enol isomers in the gas-phase, Table (1), shows an electronic energy difference in favor of the 2-hydroxypyridine form.

Table 1: Experimental data: Tautomeric equilibrium of the 2-hydroxypyridine/2-pyridone in the gas-phase, argon and nitrogen matrices. The energy in kJ/mol, T in Kelvin, and [HY]:[PY] as the ratio of the concentration at equilibrium.

ΔE	ΔH	ΔG	[HY]:[PY]	T	Method	Ref.
gas ($\varepsilon = 1.0$):						
-2.1(0.6)	-3.0(0.6)	-	2.2 : 1	473	Infrared	17
	1.3(1.3)	-3.3	2.5 : 1	405	UV	16
	-3.2(0.4)	-	3 : 1	356	Microwave	21
	-	5.4	-	298	Basicity	22
	-	-2.4(0.3)	2 : 1	403	X-ray PES	18
	-2.5(0.4)	-	4 : 1	323	PES	19
	-	-	2 : 1	503	Infrared	23
in Ar matrix:						
	-	-2.9(0.5)	2.80 : 1	340	Infrared	17
	-	-	3.03 : 1	303	Infrared	24
in N ₂ matrix:						
	-	-	2.99 : 1	340	Infrared	17
in H ₂ O ($\varepsilon = 78.36$):						
	-	15.5	-	298	Basicity	22
	14.2	-	-	298	ΔH_{soln}	25
	-	16.9	1 : 910	293	pK _a	26

Theoretical studies performed at semiempirical, density functional theory (DFT) and ab initio level of theory have attempted to predict the relative stability of the 2-pyridone/2-hydroxypyridine system in the gas-phase and solution.^{10,27,28} A coalescence of three decades of theoretical calculations on the tautomeric equilibrium by DFT and ab initio, Figure (2), shows that a quantitative agreement with the tautomerization energy is a challenge.

Although theoretical methods at different levels predict planarity in the ground-state geometries of 2-PY/2-HY isomers, as measured,^{20,21} the choice of a reliable approach is still

required for an accurate relative energetic description, and we show that modeling is sensitive to the level method used to determine the structures.

The tautomerism of the 2-pyridone/2-hydroxypyridine represented a reliability test for DFT method. The density functional theory provides good agreement with the experimental vibrational frequencies and rotational constants, but considered inherently wrong with regard to the relative stability of different tautomers.^{10,29,34,35}

The accuracy of the tautomerism energy by DFT functionals, vide Figure (2), can be ordered as B3PW91 > B3LYP > BP86 > PBE > HCTH407 = BLYP. The hybrid DFT methods, in which the functional contains an amount of Hartree-Fock (HF) exchange, prove to be superior to pure DFT functionals HCTH407, PBE, BP86 and BLYP. The B3LYP model gives a wrong sign for ΔE , even so, provides better results than the non-hybrid ones. The BHandLYP is the only one that predicts the correct tautomeric order, the 2-hydroxypyridine molecule as the most stable form in the gas-phase. Its similar performance with HF for the tautomers of pyridone and formamide¹⁰ state that the outcome for energetic stability is due the effects of the large percentage of HF exchange in the functional. Despite the reasonable estimate, the BHandLYP functional gives rotational constants in poor agreement with the experimental values.³⁵

Hartree-Fock (HF) calculation gives a modest estimation of tautomeric energy with TZV(2df,2dp) basis set, albeit inferior on molecular constants.^{10,29,32} The Hartree-Fock/6-311G(d,p) calculation gives a $\Delta E_{HF} = -4.97$ kJ/mol using the optimal geometry of the same method,³² and $\Delta E_{HF} = -7.13$ kJ/mol when the structure used is optimized by MP2,³³ data not included in Figure (2). The comparison reveals that HF grossly overestimates the tautomeric energy when employed geometric parameters closer of the experimental measurements. We should expect a similar behavior from BHandLYP functional.

The second-order Moller-Plesset perturbation (MP2) method with Pople basis set which includes p-polarization functions on hydrogens or TZV(2df,2dp) overestimates the predominance of 2-hydroxypyridine in the gas-phase.^{10,32} The spin-component-scaled Moller-Plesset

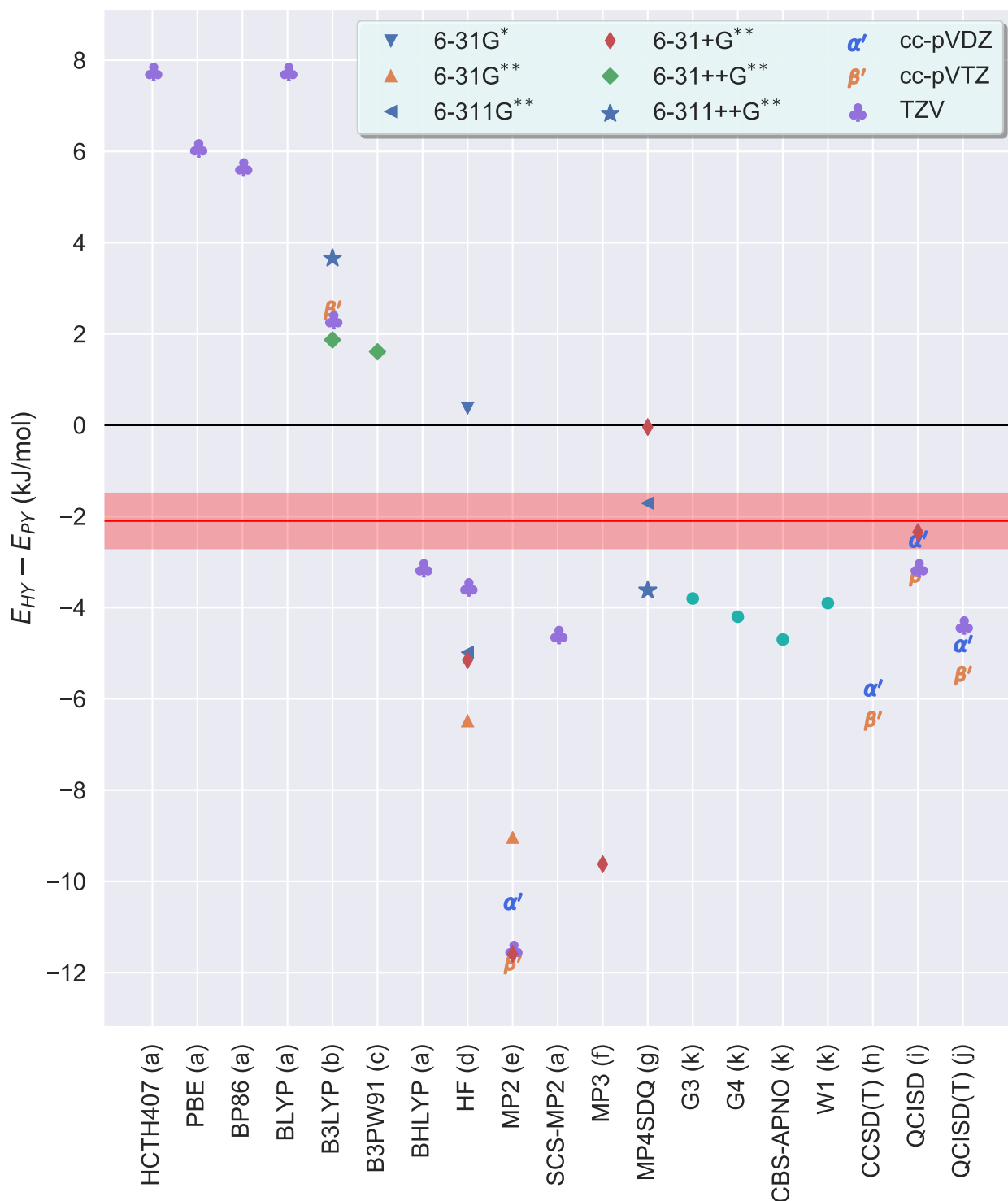


Figure 2: Results of three decades: Relative electronic energies, without zero point correction, of the 2-hydroxypyridine with respect to 2-pyridone in the gas-phase calculated by quantum methods. The correspondent experimental, $\Delta E = -2.1(0.6)$ kJ/mol, in red.¹⁷ Data from: (a, b, d, e, i, j),¹⁰ (b, c),²⁹ (b, e, h, i, j),³⁰ (b, g),³¹ (d, e, f, g, i),³² (g),³³ (k).³⁴

theory (SCS-MP2) increased the energetic accuracy compared to standard MP2 and MP3. The fourth order (MP4) proved to be the most accurate among Moller-Plesset perturbation methods, see Figure (2), although the dependence of the basis set size on the reliability of its results to represent a disadvantage due to computational cost.

Quantum chemistry composite methods G3, G4, CBS-APNO, and W1 were employed to explain the gas- and solution-phase tautomerization reaction energetics.³⁴ Compound techniques, combined methods with different levels of theory and basis set, led to an improvement on the estimation of the 2-PY/2-HY relative stability when compared with other post-HF methods, e.g. MP2, MP3 and CCSD(T).

Quadratic configuration interaction with single and double excitations (QCISD) method accurately predicts the energy differences in the gas-phase with basis sets cc-pVDZ and 6-31+G(d,p),^{30,32} but deviates of the experimental measurements when the basis set is increased to cc-pVTZ and TZV. Despite its accuracy to be a reference for other methods presented in Figure (2), the QCISD method is computationally very expensive.

In this work, our study sheds light on the fundamental features of tautomeric systems and suggests how to proceed to predict the most stable form. The long-range-corrected (LC) exchange plays a role in the accurate description of geometrical parameters, rotational constant, dipole moment, ionization potential, energy barrier and tautomeric equilibrium of the 2-pyridone/2-hydroxypyridone. We compare the DFT results with the reference wavefunction method QCISD/aug-cc-pVTZ. In the Section 2, we present the theoretical methods, the bond distances and angles, rotational constants and dipole momentum in comparative with experimental measurements are shown in the Section 3. Among our DFT functionals, we emphasize the TPSSP86 in the study of the rotational constants, dipole moments and tautomeric energy. The Section 4 explain how the long-range correction fixes the relative stability prediction. In the end, Section 5, we address the tautomerization energy to the 2-PY/2-HY system by several functionals and others tautomers with focus given to the relative stabilities in the gas-phase, which offers unique opportunities to review the reliability

of the density functional theory method. The DELTAGAUSS software, a tool developed for the calculation of relative energies, is shown in the supporting information.

2 Computational details

We calculate with GAUSSIAN 09 (G09) suite of programs that enable the reproducibility of the results provided by the same functional specification and code. Our results are by QCISD method and long-range corrected DFT functionals. Since the exchange and correlation functionals are in principle independent, we use different combinations given by concatenating the acronym of the exchange [PKZB, O, BRX, G96, TPSS, B, S, XA, PBE, PW91] with correlation functionals [B95, P86, VP86, TPSS, PKZB, PW91, BRC, LYP, PL, VWN5, KCIS, PBE], as well as the standalone [M06L, M11L, B97D, HCTH407] and exchange-only functionals [HFB, HFS, XAlpha]. The basis sets vary in complexity from 6-31++G(d,p) to aug-cc-pVQZ.

The non-Coulomb part of the functionals generally dies off too fast, i.e., becomes inaccurate at large distances, and long-range correction fixes the asymptotic limit for the exchange interaction.³⁶ The correction supplements the long-range exchange effect by replacing the Hartree-Fock exchange integral with the long-range part of exchange functionals in Kohn-Sham density functional.³⁷ The prefix LC- applies the long-range correction,³⁸ where we set the LC parameter as $\omega = 0.47$, the G09 default, with exception to M11L ($\omega = 0.25$), and other amounts as $\omega = 0.04$ with the *iop*(3/107 = 0040000000, 3/108 = 0040000000) keyword.

Our calculations are in the gas-phase and we process the results through DELTAGAUSS software. Except as otherwise indicated, we optimize all structures on internal coordinates for each functional and basis set.

3 Geometric and spectroscopic data

The experimental-theoretical geometrical parameters in the solid state of 2-pyridone and 6-chloro-2-hydroxypyridine are in Tables 2 and 3, respectively, carried out with QCISD and TPSSP86 DFT functional with and without long-range correction (LC). A theoretical-experimental comparison to the substituted hydroxypyridine allows us to estimate the validity of 2-HY geometrical parameters since is not possible to find 2-hydroxypyridine in the crystal state.³⁹ The X-ray crystal results belong to hydrogen-bonded dimers while the calculations, refer to gas-phase monomers, so a variation up to 0.02 Å is expected between theory and experiment.²⁷

Geometric predictions of the 2-pyridone and 6-chloro-2-hydroxypyridine shows a good agreement with experiments, an indicative of the reliability of 2-hydroxypyridine optimal geometry. The inclusion of long-range correction with $\omega = 0.04$ in the functionals does not have a significant impact on bond lengths and angles in comparison to pure ones, whereas with $\omega = 0.47$ tend to Hartree-Fock results. The 2-PY structure predicted by QCISD is closer to HF than our chosen meta-GGA functional.

The bond lengths of the transition state (TS), see Table (4), are intermediaries between the bond distances of the 2-PY (Table (2)) and 2-HY (Table (3)). Yet, as noted by Moreno et al.,⁴² the TS bond angles are non-intermediaries values of the two minima, wherein is necessary a significant decrease of the angle $\angle \text{OC}_1\text{N}$ to allow the intramolecular tautomerism. This profound change in the angles involved in the H-atom transfer explains the high energetic barrier of the tautomers, shown in Section 5.

It is important to highlight the nonplanarity failures of MP2, MP3, CISD, and CCSD ab initio methods with popular basis sets on arenes,⁴³ which arise from an adverse intramolecular basis set incompleteness error (BSIE). Our calculations by post-HF methods with Pople basis set, of geometry by MP2/aug-cc-pVDZ, provides: 2-pyridone has at least one sizable imaginary vibrational frequency at MP2/6-311G ($225i \text{ cm}^{-1}$, A"; $65i \text{ cm}^{-1}$, A"), MP3/6-

Table 2: Experimental geometrical parameters of the 2-pyridone (2-PY) in the solid phase, first column, from ref. ⁴⁰ Our geometric optimization results of the 2-PY (gas-phase) by QCISD, Hartree-Fock and our TPSSP86 DFT functional with aug-cc-pVTZ basis set excepting for ω' , performed with cc-pVTZ. Pure functional is the case where the long-range correction parameter is $\omega = 0$. Units: Angles in Degrees and r in Å.

	2-PY	gas (theory) 2-pyridone					
	solid (exp.)	QCISD	Pure	$\omega(0.04)$	$\omega'(0.04)$	$\omega(0.47)$	HF
$r(\text{N}-\text{C}_1)$	1.379	1.393	1.419	1.415	1.417	1.377	1.379
$r(\text{C}_1-\text{C}_2)$	1.437	1.456	1.448	1.445	1.445	1.439	1.455
$r(\text{C}_2-\text{C}_3)$	1.370	1.357	1.369	1.368	1.367	1.338	1.339
$r(\text{C}_3-\text{C}_4)$	1.416	1.433	1.424	1.421	1.422	1.418	1.435
$r(\text{C}_4-\text{C}_5)$	1.366	1.353	1.366	1.365	1.365	1.336	1.335
$r(\text{C}_1-\text{O})$	1.250	1.223	1.233	1.232	1.230	1.211	1.199
$r(\text{N}-\text{H}_1)$	1.034	1.007	1.016	1.016	1.016	1.009	0.993
$r(\text{C}_2-\text{H}_2)$	1.088	1.080	1.085	1.085	1.085	1.079	1.071
$r(\text{C}_3-\text{H}_3)$	1.088	1.082	1.088	1.088	1.088	1.082	1.074
$r(\text{C}_4-\text{H}_4)$	1.087	1.078	1.083	1.083	1.083	1.077	1.069
$r(\text{C}_5-\text{H}_5)$	1.083	1.080	1.085	1.085	1.085	1.080	1.071
$\angle \text{NC}_1\text{C}_2$	114.97	113.52	112.90	112.95	112.78	113.69	113.86
$\angle \text{C}_1\text{C}_2\text{C}_3$	121.07	121.42	121.72	121.68	121.78	121.20	120.98
$\angle \text{C}_2\text{C}_3\text{C}_4$	120.97	121.31	121.58	121.57	121.58	121.55	121.52
$\angle \text{C}_3\text{C}_4\text{C}_5$	117.77	117.89	118.09	118.06	118.03	117.72	117.58
$\angle \text{OC}_1\text{N}$	120.23	120.46	119.63	119.58	119.63	120.08	120.48
$\angle \text{H}_1\text{NC}_1$	117.95	114.69	114.27	114.11	114.00	114.30	115.11
$\angle \text{H}_2\text{C}_2\text{C}_1$	120.25	116.24	116.34	116.31	116.23	116.30	116.49
$\angle \text{H}_3\text{C}_3\text{C}_2$	119.28	119.58	119.46	119.45	119.46	119.42	119.59
$\angle \text{H}_4\text{C}_4\text{C}_3$	122.24	121.66	121.64	121.68	121.67	121.69	121.54
$\angle \text{H}_5\text{C}_5\text{C}_4$	125.62	123.50	123.66	123.63	123.60	123.24	123.03

Table 3: Experimental data, from ref.,⁴¹ and theoretical (DFT) geometrical parameters of the 6-chloro-2-hydroxypyridine (6-chloro-2-HY) in solid and gas-phase, first and second column, respectively. Our calculations for 2-HY by QCISD, Hartree-Fock and TPSSP86 DFT functional with aug-cc-pVTZ basis set excepting for ω' , performed with cc-pVTZ. Pure functional is the case where the long-range correction parameter is $\omega = 0$. Units: Angles in Degrees and r in Å.

	6-chloro-2-HY		gas (theory) 2-hydroxypyridine					
	solid (exp.)	$\omega(0.04)$	QCISD	Pure	$\omega(0.04)$	$\omega'(0.04)$	$\omega(0.47)$	HF
$r(\text{N}-\text{C}_1)$	1.341	1.334	1.321	1.332	1.330	1.331	1.305	1.304
$r(\text{C}_1-\text{C}_2)$	1.393	1.398	1.400	1.402	1.400	1.400	1.383	1.394
$r(\text{C}_2-\text{C}_3)$	1.377	1.388	1.381	1.388	1.386	1.386	1.364	1.369
$r(\text{C}_3-\text{C}_4)$	1.382	1.396	1.399	1.401	1.398	1.399	1.382	1.391
$r(\text{C}_4-\text{C}_5)$	1.362	1.389	1.383	1.390	1.388	1.388	1.367	1.371
$r(\text{C}_1-\text{O})$	1.321	1.354	1.352	1.362	1.358	1.357	1.335	1.332
$r(\text{C}_5-\text{Cl})$	1.739	1.753	-	-	-	-	-	-
$r(\text{O}-\text{H}_1)$	1.009	0.977	0.964	0.977	0.977	0.977	0.965	0.944
$r(\text{C}_2-\text{H}_2)$	0.974	1.084	1.080	1.085	1.085	1.085	1.079	1.071
$r(\text{C}_3-\text{H}_3)$	0.925	1.086	1.082	1.087	1.087	1.087	1.082	1.074
$r(\text{C}_4-\text{H}_4)$	1.020	1.083	1.080	1.085	1.085	1.085	1.079	1.071
$r(\text{C}_5-\text{H}_5)$	-	-	1.083	1.088	1.088	1.088	1.083	1.074
$\angle \text{NC}_1\text{C}_2$	122.05	123.94	124.41	124.30	124.32	124.30	123.98	123.87
$\angle \text{C}_1\text{C}_2\text{C}_3$	118.44	117.10	117.35	117.26	117.26	117.28	117.31	117.26
$\angle \text{C}_2\text{C}_3\text{C}_4$	120.06	120.32	119.47	119.63	119.61	119.62	119.69	119.74
$\angle \text{C}_3\text{C}_4\text{C}_5$	116.94	116.63	117.96	118.09	118.11	118.07	117.91	117.51
$\angle \text{OC}_1\text{N}$	118.57	116.83	117.47	116.96	116.90	116.83	117.29	117.88
$\angle \text{H}_1\text{OC}_1$	116.14	106.09	106.17	105.61	105.40	105.00	106.72	108.56
$\angle \text{NC}_5\text{Cl}$	114.79	116.13	-	-	-	-	-	-
$\angle \text{H}_2\text{C}_2\text{C}_1$	117.50	120.32	119.97	120.26	120.19	120.14	119.85	120.06
$\angle \text{H}_3\text{C}_3\text{C}_2$	121.13	119.95	120.05	119.91	119.93	119.92	119.94	119.93
$\angle \text{H}_4\text{C}_4\text{C}_3$	125.23	122.45	121.51	121.37	121.39	121.39	121.55	121.67
$\angle \text{H}_5\text{C}_5\text{C}_4$	-	-	120.79	121.05	121.03	120.98	120.82	120.59

Table 4: Geometrical parameters of the 2-pyridone/2-hydroxypyridine transition state (TS) in the gas-phase. Our geometric optimizations by Hartree-Fock and TPSSP86 DFT functional with aug-cc-pVTZ basis set excepting for ω' , performed with cc-pVTZ. Pure functional is the case where the long-range correction parameter is $\omega = 0$. Units: Angles in Degrees and r in Å.

	gas (theory) transition state of 2-PY/2-HY				
	Pure	$\omega(0.04)$	$\omega'(0.04)$	$\omega(0.47)$	HF
$r(\text{N}-\text{C}_1)$	1.369	1.367	1.368	1.338	1.335
$r(\text{C}_1-\text{C}_2)$	1.410	1.407	1.408	1.393	1.403
$r(\text{C}_2-\text{C}_3)$	1.389	1.387	1.386	1.362	1.366
$r(\text{C}_3-\text{C}_4)$	1.410	1.407	1.407	1.395	1.407
$r(\text{C}_4-\text{C}_5)$	1.389	1.387	1.386	1.361	1.365
$r(\text{C}_1-\text{O})$	1.298	1.295	1.294	1.273	1.266
$r(\text{O}-\text{H}_1)$	1.383	1.382	1.382	1.353	1.330
$r(\text{N}-\text{H}_1)$	1.302	1.299	1.299	1.274	1.270
$r(\text{C}_2-\text{H}_2)$	1.084	1.084	1.084	1.078	1.069
$r(\text{C}_3-\text{H}_3)$	1.088	1.087	1.087	1.082	1.074
$r(\text{C}_4-\text{H}_4)$	1.084	1.084	1.084	1.078	1.070
$r(\text{C}_5-\text{H}_5)$	1.086	1.085	1.085	1.081	1.072
$\angle \text{NC}_1\text{C}_2$	120.19	120.17	120.05	120.38	120.75
$\angle \text{C}_1\text{C}_2\text{C}_3$	116.59	116.58	116.64	116.26	115.95
$\angle \text{C}_2\text{C}_3\text{C}_4$	122.09	122.12	122.13	122.32	122.32
$\angle \text{C}_3\text{C}_4\text{C}_5$	118.77	118.75	118.71	118.39	118.07
$\angle \text{OC}_1\text{N}$	105.34	105.40	105.50	105.58	105.16
$\angle \text{H}_1\text{OC}_1$	74.99	74.93	74.88	74.63	74.97
$\angle \text{H}_1\text{NC}_1$	75.34	75.32	75.23	75.11	74.65
$\angle \text{H}_2\text{C}_2\text{C}_1$	120.94	120.93	120.86	120.85	121.08
$\angle \text{H}_3\text{C}_3\text{C}_2$	119.02	119.00	118.99	118.93	119.00
$\angle \text{H}_4\text{C}_4\text{C}_3$	121.02	121.04	121.05	121.13	121.15
$\angle \text{H}_5\text{C}_5\text{C}_4$	123.39	123.37	123.36	123.09	122.72

Table 5: Rotational constants, in MHz, and dipole moments, in Debye, of the 2-hydroxypyridine (2-HY) and 2-pyridone (2-PY). ^(a)Exp. data from ref. ²⁹ Our theoretical results in the gas-phase by QCISD and TPSSP86 DFT functional with aug-cc-pVTZ basis set excepting for $\tilde{\omega}$ $\bar{\omega}$ and $\hat{\omega}$, performed respectively with aug-cc-pVDZ, 6-311++G(2d,2p) and aug-cc-pVQZ. The pure functional is with LC parameter $\omega = 0$.

		TPSSP86							
	Exp. ^(a)	QCISD	Pure	$\omega(0.04)$	$\omega(0.26)$	$\omega(0.47)$	$\tilde{\omega}(0.04)$	$\bar{\omega}(0.04)$	$\hat{\omega}(0.04)$
2-HY:									
<i>A</i>	5824.9459(44)	5860.42	5805.98	5822.59	5898.08	6000.60	5753.34	5813.79	5825.84
<i>B</i>	2767.5307(20)	2779.42	2752.14	2763.46	2801.38	2840.68	2741.46	2760.92	2765.35
<i>C</i>	1876.1647(17)	1885.29	1867.10	1874.03	1899.28	1927.98	1856.73	1871.95	1875.23
μ	1.39(3)	1.53	1.32	1.31	1.38	1.41	1.34	1.35	1.31
2-PY:									
<i>A</i>	5643.7585(15)	5677.58	5643.20	5664.30	5731.55	5799.52	5610.19	5654.57	5666.35
<i>B</i>	2793.47174(98)	2802.16	2767.36	2777.16	2818.72	2868.22	2751.12	2774.39	2779.48
<i>C</i>	1868.82345(99)	1876.18	1856.80	1863.50	1889.49	1919.10	1845.92	1861.20	1864.77
μ	4.26(24)	4.79	4.30	4.30	4.38	4.45	4.35	4.35	4.29

311++G (798*i* cm⁻¹, A^{''}; 39*i* cm⁻¹, A^{''}), MP4/6-311++G (838*i* cm⁻¹, A^{''}; 161*i* cm⁻¹, A^{''}); on 2-hydroxypyridine gives: MP2/6-311++G (559*i* cm⁻¹, A^{''}), MP3/6-311++G (471*i* cm⁻¹, A^{''}), MP4/6-311++G (533*i* cm⁻¹, A^{''}). Independent of the method applied to 2-PY/2-HY system, the correlation-consistent (aug)-cc-pVXZ basis sets, that provide the necessary BSIE balance,⁴³ are good choices in this regard.

The microwave spectroscopic study of the 2-PY/2-HY equilibrium in the gas-phase provided both the rotational constants and the dipole moments for the two isomers in question.²⁹ The spectroscopic data are presented in Table (5) along with the predicted quantities at QCISD and DFT level. We note a better accordance between experiments and theory with the inclusion of the long-range correction with parameter $\omega = 0.04$. The root-mean-square errors (r.m.s) of the theoretical rotational constants in Table (5) for 2-hydroxypyridine are 22, 15, 3 and 114 MHz by QCISD, pure TPSSP86, LC-TPSSP86 with $\omega = 0.04$ and $\omega = 0.47$, respectively, while for 2-PY the r.m.s are 21, 17, 15 and 104 MHz.

Rotational constant results with $\omega = 0.04$ parameter long-range exchange exceed the accuracies of our computation by QCISD/aug-cc-pVTZ and MP2 approaches with Pople

Table 6: Spectroscopic data of the 2-hydroxypyridine (2-HY) and 2-pyridone (2-PY). A , B and C are rotational constants in megahertz; μ , dipole moment in Debye, ^(a)experimental data from ref. ²⁹ Our theoretical results in the gas-phase by TPSSP86 DFT functional with may-, jun-, jul-, aug- cc-pVTZ basis sets. The long-range correction parameter $\omega = 0.04$.

		LC-TPSSP86 $\omega(0.04)$				
	Exp. ^(a)	cc-	may-cc-	jun-cc-	jul-cc-	aug-cc-
2-HY:						
A (MHz)	5824.9459(44)	5822.26	5821.94	5822.00	5822.81	5822.59
B (MHz)	2767.5307(20)	2764.70	2763.14	2763.20	2763.49	2763.46
C (MHz)	1876.1647(17)	1874.57	1873.82	1873.85	1874.06	1874.03
μ (D)	1.39(3)	1.17	1.33	1.31	1.31	1.31
2-PY:						
A (MHz)	5643.7585(15)	5665.31	5663.78	5663.79	5664.40	5664.30
B (MHz)	2793.47174(98)	2775.89	2776.43	2776.81	2777.37	2777.16
C (MHz)	1868.82345(99)	1863.04	1863.12	1863.29	1863.61	1863.50
μ (D)	4.26(24)	4.15	4.35	4.30	4.30	4.30

basis set, cf. MP2 results.^{29,33} As the parameter ω increases, the estimated constants tend to be closer to that predicted by HF²⁹ overestimating the rotational constants of the 2-PY/2-HY molecules. The inclusion of diffuse functions gives a significant improvement in the dipole moment of the 2-hydroxypyridine, see Table (6), and thereby plays a relevant role on solvation. Accurate calculations of electrical properties also need augmented basis sets for accurate calculations.⁴⁴ The addition of the dispersion function in the basis set, especially aug-cc-pVTZ, provides reliable results with a small difference to the given by a bigger basis set, aug-cc-pVQZ, indicating a quick convergence to the same value of the complete basis set (CBS) limit with respect to geometric parameters, dipole moment and rotational constants.

Predictions by LC-TPSSP86 functional, $\omega = 0.04$, with aug-cc-pVDZ and 6-31++G(d,p) basis sets underestimates the rotational constants in comparative to experiments, Table (5). The results with 6-311++G(2d,2p) basis set, indicated by cost-effective for optical rotation calculations of two simple chiral molecules,^{45,46} agree to the aug-cc-pVTZ, but as will see in Section 5 the same augmented Pople basis to overestimate the tautomeric energy.

Table 7: Theoretical results of the rotational constants and dipole moment of the 2-hydroxypyridine (2-HY) and 2-pyridone (2-PY) in the gas-phase. Our calculations by exchange-correlation (Exc-Cor) energy functionals in density functional theory (DFT) with aug-cc-pVTZ basis and long-range correction parameter $\omega = 0.04$.

Exchange:	TPSS			B		BRX	
Correlation:	PKZB	TPSS	PW91	KCIS	PW91	KCIS	PW91
2-HY:							
$A(\text{MHz})$	5829.13	5830.77	5835.48	5825.15	5827.14	5820.53	5822.47
$B(\text{MHz})$	2765.08	2766.05	2767.65	2759.97	2763.96	2754.71	2758.64
$C(\text{MHz})$	1875.45	1876.07	1877.29	1872.69	1874.73	1869.79	1871.80
$\mu(\text{D})$	1.29	1.28	1.30	1.22	1.23	1.26	1.28
2-PY:							
$A(\text{MHz})$	5671.02	5672.78	5676.32	5662.54	5666.71	5654.50	5658.34
$B(\text{MHz})$	2778.75	2779.53	2781.76	2773.99	2777.22	2772.32	2775.40
$C(\text{MHz})$	1864.95	1865.49	1866.87	1861.88	1863.79	1860.26	1862.06
$\mu(\text{D})$	4.28	4.27	4.29	4.21	4.27	4.34	4.36

4 The Koopmans’ theorem

The HOMO energy (ε_{HOMO}) and ionization potential (IP) are the most important quantities to explain why the pure DFT prediction, shown in Figure (2), is inherently wrong with regard to the relative stability order of the proton-transfer tautomerism. The energy difference between the neutral and radical species, without the geometric relaxation, defines the vertical ionization potential (vIP). The experimental vIPs are 879.10 and 831.72 kJ/mol for 2-hydroxypyridine and 2-pyridone, respectively.⁴⁷

The vertical IPs of the 2-hydroxypyridine and 2-pyridone by TPSSP86 with several long-range correction parameters, shown in Table (8). The same functional with $\omega = 0.00$ (pure) and $\omega = 0.04$ yields good structures (Section 3) but underestimates the vIP, while the predictions with relaxed structures by $\omega = 0.26$ and $\omega = 0.47$ overestimates the measurements. We achieve the smallest deviation in $\Delta(\text{vIP}_{teo-exp})$ by $\omega^* = 0.25$ and $\omega^* = 0.26$ where the asterisk means that we calculate from a reliable geometry, i.e., with $\omega = 0.04$. Koopmans’ theorem, which states $\text{IP} = -\varepsilon_{HOMO}$, allows us a comparison between the first ionization energy and the orbital energy of the highest occupied molecular orbital (HOMO). We define

Table 8: Theoretical and experimental vertical ionization potentials (vIP) of the 2-hydroxypyridine (2-HY) and 2-pyridone (2-PY). Our results in the gas-phase by QCISD and TPSSP86 DFT functional with aug-cc-pVTZ basis sets. The calculations are in kJ/mol and from relaxed geometry, except for ω^* , wherein the long-range correction parameter $\omega = 0.04$ define the structures. The $\Delta(\text{vIP}_{teo-exp})$ is the accuracy of our results, cf. exp. data of the ref.,⁴⁷ and ε_{HOMO} is the HOMO energy. When $\Delta K_{teo} = 0$, fulfills Koopmans’ theorem. $(E_{HY} - E_{PY})$ is the estimated tautomeric energy, cf. $\Delta E_{exp} = -2.1(6)$ kJ/mol. $\Delta\varepsilon_{HOMO}$ is the difference between the $-\varepsilon_{HOMO}$ of each tautomer.

	$-\varepsilon_{HOMO}$	vIP_{teo}	$\Delta(\text{vIP}_{teo-exp})$	ΔK_{teo}	$\parallel (E_{HY} - E_{PY})$	$\Delta\varepsilon_{HOMO}$
2-HY:						
$w(0.00)$	583.84	856.80	-22.30	272.96	5.70	42.79
$w(0.04)$	640.83	856.76	-22.34	215.93	4.69	42.83
$w(0.26)$	873.42	888.89	9.79	15.47	-1.30	48.43
$w(0.47)$	953.21	901.81	22.71	-51.40	-1.20	47.27
$w^*(0.25)$	867.06	887.17	8.06	20.11	-1.49	49.81
$w^*(0.26)$	873.31	888.32	9.20	15.01	-1.65	50.15
$w^*(0.47)$	951.51	899.16	20.06	-52.35	-2.66	52.50
QCISD	871.73	868.04	-11.06	-3.69	-1.50	36.47
HF	870.54	746.75	-132.35	123.79	-3.28	32.36
2-PY:						
$w(0.00)$	541.05	810.15	-21.57	269.10		
$w(0.04)$	598.00	810.08	-21.64	212.08		
$w(0.26)$	824.99	840.25	8.53	15.26		
$w(0.47)$	905.94	855.37	23.65	-50.57		
$w^*(0.25)$	817.25	836.73	5.01	19.48		
$w^*(0.26)$	823.16	837.70	5.98	14.54		
$w^*(0.47)$	899.01	846.26	14.54	-52.75		
QCISD	835.26	822.48	-9.24	-12.78		
HF	838.18	693.85	-137.87	144.33		

$\Delta K_{teo} = \text{IP} + \varepsilon_{HOMO}$, in which $\Delta K_{teo} = 0$ fulfills Koopmans’ theorem. The pure TPSSP86 functional or with a small long-range parameter, $\omega = 0.04$, presents the largest deviations of the theorem, while the increment in ω , especially $\omega^* = 0.26$, tend to fulfill. The reason why long-range correction enhances the reproducibility of HOMO energy is due to the orbital energies almost constant for fractional occupied orbitals.^{37,48,49}

QCISD method results as well exhibits small ΔK_{teo} . Despite the large deviation of the ΔK_{teo} by Hartree-Fock calculation, in the account of wrong vIP prediction, the $-\varepsilon_{HOMO}$ is close to the experimental vIP what explains the correct order estimation on the relative

stability of the 2-PY/2-HY tautomeric forms.

The difference between the $-\varepsilon_{HOMO}$ of each tautomer, $\Delta\varepsilon_{HOMO}$, reveals the other piece of the puzzle for a quantitative estimation of the relative stability. We highlight the robust correlation between $\Delta\varepsilon_{HOMO}$ and ΔE results by DFT in Table (8). Despite LC-TPSSP86 with $\omega^* = 0.47$ dissatisfy the Koopmans’ theorem, the long-range exchange interaction pushes the orbitals up consistently, while the ΔE cancels the total energy error. The use of reliable structures becomes the key to this achievement. The same argument explains why $\Delta E_{\omega^*=0.25}$, calculation from a good structure ($\omega = 0.04$), is closer to experimental results than $\Delta E_{\omega=0.26}$, albeit the $\omega^* = 0.25$ to provide a bigger deviation in ΔK_{teo} .

The Figure (3) shows the effect on electron density of the 2-PY/2-HY due the inclusion long-range correction. There is a redistribution of electrons (blue), specially from hydrogen, to carbon atoms.

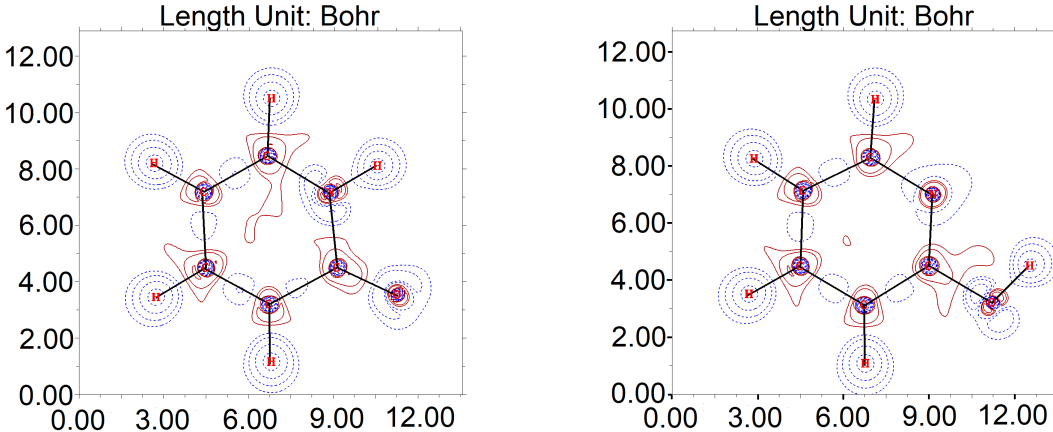


Figure 3: Difference map of electron density 2-pyridone (left) and 2-hydroxypyridine (right) when we include long-range correction. The contour lines with isovalue (magnitude starts at 0.001 a.u.) in red solid lines and blue dashed lines correspond to the regions with increased electron density and decreased electron density, respectively, due LC-parameter $\omega^* = 0$ to $\omega^* = 0.26$ in TPSSP86/aug-cc-pVTZ.

Table 9: Relative energies in kJ/mol from the relaxed geometry of the 2-pyridone (2-PY) \rightarrow 2-hydroxypyridine (2-HY), except for ω^* , where we calculate the structures with long-range correction parameter $\omega = 0.04$. Experimental data from ^(a) ref. ¹⁷ and ^(b) ref. ²¹ Our theoretical results in gas-phase at room temperature (298.15 K) by QCISD, Hartree-Fock and TPSSP86 DFT functional with aug-cc-pVTZ basis set excepting for $\tilde{\omega}$ and $\bar{\omega}$, performed respectively with aug-cc-pVDZ and 6-311++G(2d,2p). Pure functional: $\omega = 0$.

		TPSSP86							HF
	Exp.	QC	Pure	$\omega^*(0.26)$	$\omega^*(0.47)$	$\omega(0.47)$	$\tilde{\omega}^*(0.47)$	$\bar{\omega}^*(0.47)$	
ΔE	-2.1(0.6) ^(a)	-1.5	5.70	-1.65	-2.66	-1.20	-4.07	-4.06	-3.28
ΔH	-3.2(0.4) ^(b)		4.97	-2.45	-3.65	-2.27	-4.98	-4.77	-4.38
ΔG	-2.9(0.5) ^(a)		5.49	-2.10	-3.34	-1.79	-4.66	-4.38	-3.84
Δzpc	-0.9 ^(a)		-0.57	-0.69	-0.86	-0.94	-0.77	-0.53	-0.94
ΔE^z			5.13	-2.34	-3.52	-2.14	-4.85	-4.60	-4.22
$-T\Delta S$			0.52	0.35	0.31	0.49	0.32	0.39	0.54
ΔE^\ddagger			138.81	130.83	151.17	151.18			210.05
ΔH^\ddagger			124.99	117.60	136.80	137.28			194.69
ΔG^\ddagger			126.20	118.75	137.82	138.54			195.94

Table 10: Tautomeric free energy in gas-phase and water, in kJ/mol, of the 2-pyridone (2-PY) \rightarrow 2-hydroxypyridine (2-HY), except for ω^* , wherein we calculate the structures with long-range correction parameter $\omega = 0.04$. Our theoretical results are with structures in gas-phase and aug-cc-pVTZ basis set. Pure functional: $\omega = 0$. Experimental data from ^(a) ref., ¹⁷ $T = 340$ K, and ^(b) the mean value of ref. ²⁶ and ref., ²² $T = 298$ K.

		TPSSP86				
	Exp.	Pure	$\omega^*(0.26)$	$\omega^*(0.47)$	$\omega(0.47)$	HF
$\Delta G(gas)$	-2.9(0.5) ^(a)	5.56	-2.05	-3.29	-1.72	-3.76
$\Delta G(water)$	16.2(0.7) ^(b)	22.71	15.84	15.75	16.75	15.66

5 Tautomeric energies and charge distributions

Various levels of theory was applied to estimate the tautomeric energy of the 2-pyridone and 2-hydroxypyridine, but none of the methods shown a quantitative result of the relative stability, see Figure (2). We report in Table (9) the relative energies at 298 K considering the effect of basis set and long-range exchange interaction on 2-PY/2-HY system. The total energies is in Table (13). The inclusion of the long-range parameter $\omega^* = 0.26$ ($\omega^* = 0.47$) in TPSSP86/aug-cc-pVTZ yields a relative energy $\Delta E_{\omega^*(0.26)} = -1.65$ kJ/mol ($\Delta E_{\omega^*(0.47)} =$

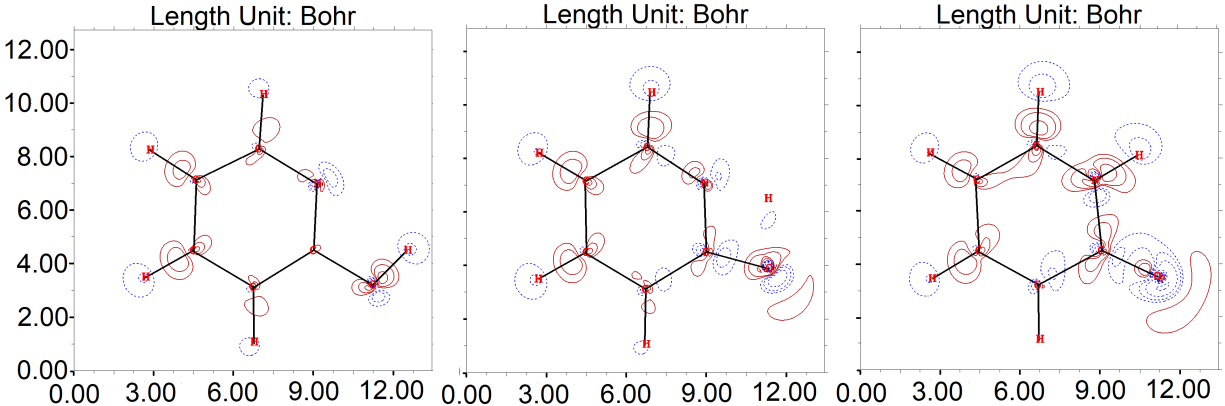


Figure 4: Map of electron density differences of the 2-hydroxypyridine, transition state and 2-pyridone in relation to gas-phase and polar medium (water). The contour lines in red solid lines and blue dashed lines correspond to the regions with increased electron density and decreased electron density. We use Multiwfn,⁵⁰ 1-3-5 plane of carbon atoms. Method: $\omega^* = 0.26$ in TPSSP86/aug-cc-pVTZ.

-2.66) in excellent agreement with experimental measurements $\Delta E_{exp} = -2.1(0.6)$ kJ/mol, where the asterisk means the use of geometric data close to the empirical one, i.e., by the inclusion of $\omega = 0.04$. When we use structures by LC-parameter $\omega = 0.47$, the G09 default, we get a decline on the relative stability $\Delta E_{\omega(0.47)} = -1.20$ kJ/mol, a non-intuitive result, since we would expect a tendency of a larger ω to the Hartree-Fock/aug-cc-pVTZ estimation, $\Delta E_{HF} = -3.28$ kJ/mol. Another notable effect of the long-range correction is on energy barrier, without zero-point energy, where our calculations establish an interval $\Delta E^\ddagger = [130.83 - 151.17]$ kJ/mol by $\omega^* = 0.26$ and $\omega^* = 0.47$, both parameters within the experimental accuracy of tautomeric energy ΔE .

The deviation of the energy values in Table (11) for not full augmented basis sets, e.g. jul-cc-pVTZ, that remove the diffuse function from hydrogens from aug-cc-pVTZ, is small in respect to full one. These basis sets also give good concordance with aug-cc-pVTZ on rotational and dipole moments as shown in Table (6). We get a clear trend of the overestimation of the 2-HY stability in absence of diffuse functions of the basis set for $\omega^* = 0.47$.

Solvation plays an active role in the reaction dynamics which influence chemical processes, e.g. tautomeric equilibrium. Once the water is the most important and abundant liquid

Table 11: Relative energies in kJ/mol of the 2-hydroxypyridine (2-HY) and 2-pyridone (2-PY). Experimental data: ^(a) ΔE from ref. ¹⁷ ^(b) ΔH at 356 K from ref. ²¹ and ^(a) ΔG at 340 K. Our theoretical results in the gas-phase at 356 Kelvin by TPSSP86 DFT functional with may-, jun-, jul-, aug- cc-pVTZ basis sets. The long-range correction parameter is $\omega^* = 0.47$ from the geometry with $\omega = 0.04$.

	Exp.	LC-TPSSP86 $\omega^*(0.47)$				
		cc-	may-cc-	jun-cc-	jul-cc-	aug-cc-
ΔE	$-2.1(0.6)^{(a)}$	-2.88	-3.09	-2.78	-2.72	-2.66
ΔH	$-3.2(0.4)^{(b)}$	-3.83	-4.00	-3.71	-3.68	-3.65
ΔG	$-2.9(0.5)^{(a)}$	-3.39	-3.59	-3.32	-3.30	-3.27
Δzpc	$-0.9^{(a)}$	-0.79	-0.76	-0.79	-0.83	-0.86
ΔE^z		-3.66	-3.85	-3.57	-3.55	-3.52
$-T\Delta S$		0.43	0.40	0.39	0.39	0.38

medium, we calculate its effect on the 2-pyridone/2- hydroxypyridine tautomeric system. To investigate the contribution of the environment, we account the implicit solvents via integral equation formalism polarizable continuum model (IEF-PCM). Despite to be an approximation, the macroscopic continuum captures physical aspects of the solvation in excellent agreement with experiments, see Table (11). The main reason for reproducibility is that in dipolar solvents the dominant term in the solute-solvent interaction is the electrostatic one. The apparent good result with Hartree-Fock is due to the prediction from low-quality geometric parameters in gas-phase by the same method.

The Figure (4) represent the effect of the solvation on electron density of the 2-hydroxypyridine, transition state and 2-pyridone. Red solid lines and blue dashed lines correspond to the regions with increased electron density and decreased electron density, respectively, going from gas-phase to polar medium (water) with $\omega^* = 0.26$ in TPSSP86/aug-cc-pVTZ. There is a notable similarity with figure 2 of Wong et al.,³² including the participation of C4 and C5 atoms and electron density in 2-PY nitrogen. However, our calculation of the transition state is the key to reveal the process of electron redistribution from H12 to C4 - C5 when 2-pyridone is the most stable form. These results indicate that an electron-withdrawing group, Cl, for example, attached to C5 atom would decrease the weight of the dipolar resonance

Table 12: Theoretical and experimental tautomeric equilibrium of the hydroxy (left) and oxo (right) forms at the respective temperature, in Kelvin. Our results by LC-TPSSP86/aug-cc-pVTZ with $\omega^* = 0.26$ at the top and $\omega^* = 0.47$ in brackets, see text. Experimental data of the formamide from ref. ²⁷ 2-pyridone from ref. ¹⁷ and from ref. ³⁰ for the 2-quinolinone, 2-pyrazinone, 2-quinoxalinone and 4-pyrimidinone. Energies in kJ/mol.

Tautomers	Theoretical			T	Experimental		
	ΔE	ΔG	[hy]:[oxo]		ΔE	ΔG	[hy]:[oxo]
	48.52 [51.79]	50.73 [53.40]	1 : 77 · 10 ⁷ [1 : 23 · 10 ⁸]	298	46.0(16.7)	—	—
	-1.65 [-2.66]	-2.05 [-3.29]	2.1 : 1 [3.2 : 1]	340	-2.1(0.6)	-2.9(0.5)	2.8 : 1
	16.19 [18.43]	15.77 [17.89]	1 : 68 [1 : 120]	450	—	17(1.5)	1 : 95
	-6.49 [-7.64]	-6.79 [-8.38]	9.7 : 1 [16 : 1]	360	—	-8.0(1.0)	14 : 1
	13.49 [16.17]	13.18 [15.61]	1 : 34 [1 : 65]	450	—	14(1.0)	1 : 40
	2.93 [2.80]	2.76 [2.29]	1 : 2.3 [1 : 2.0]	400	—	2.4(0.3)	1 : 2.1

Table 13: Total energies in Hartrees from the relaxed geometry of the 2-pyridone (2-PY) \rightarrow 2-hydroxypyridine (2-HY), except for ω^* , wherein we calculate the structures with long-range correction parameter $\omega = 0.04$. Our theoretical results in gas-phase by QCISD, Hartree-Fock and TPSSP86 DFT functional with aug-cc-pVTZ basis set. Pure functional: $\omega = 0$.

	QC	TPSSP86				HF
		Pure	$\omega^*(0.26)$	$\omega^*(0.47)$	$\omega(0.47)$	
E_{PY}	-322.93729	-323.84142	-323.33217	-323.22828	-323.23218	-321.68730
E_{HY}	-322.93786	-323.83924	-323.33280	-323.22930	-323.23263	-321.68855

form in favor of hydroxypyridine configuration, and 6-chloro-2-hydroxypyridine is exactly the most stable form in solid-phase^{39,41} and by our calculations in gas-phase.

To test if the reproduction of the experimental data on 2-PY/2-HY system by our model is only a particular case, we carry out an analogous approach for other compounds. In Table (12), we compare the results of such computations with experimental measurements. There is an excellent concordance on relative stability prediction in the gas-phase for formamide, 2-pyridone, 2-quinolinone, 2-pyrazinone, 2-quinoxalinone and 4-pyrimidinone at their respective temperatures by LC-TPSSP86/aug-cc-pVTZ with long-range parameter $\omega^* = 0.26$ and $\omega^* = 0.47$, where the asterisk means the use of a structure close to the pure DFT functional evaluation, i.e., $\omega = 0.04$. These excellent results corroborate the reliability of our description.

Table 14: Relative energies in kJ/mol from geometry, with LC parameter $\omega = 0.04$, of the 2-hydroxypyridine and 2-pyridone in the gas-phase. Our calculations by exchange-correlation (Exc-Cor) energy functionals in density functional theory (DFT) with an aug-cc-pVTZ basis set and a long-range correction parameter $\omega^* = 0.47$. ^(a)Experimental data from ref. ¹⁷

	Exp. ^(a)	Exc:	TPSS			B		BRX	
		Cor:	PKZB	TPSS	PW91	KCIS	PW91	KCIS	PW91
ΔE	-2.1(0.6)		-2.22	-2.41	-1.92	-2.39	-2.15	-2.69	-2.48

The Figures 5, 6 and 7 coalesce the estimation of the relative energy by our list of functionals in Section 2. We highlight in Table (14) the excellent agreement of the ΔE by some LC functionals with $\omega^* = 0.47$, in which the asterisk means the use of structures with

$\omega^* = 0.04$ that shows a good concordance to the measured rotational constant, see Table (7).

6 Summary and outlook

Our work sheds light on a matter of investigation which lasts more than a century, a challenge to the reliability of the quantum methods, especially to DFT. In our literary review, the QCISD method yielded the most accurate result, while the other wavefunction methods, including CCSD, tended to overestimate the predominance of the hydroxy form in the gas-phase. On the other hand, the pure density functional methods estimated the oxo form as the most stable, contradictory to the experimental measurements. Our results reveal the responsible for the notable contrast between the relative stability order estimation by wavefunction (WF) and density functional (DFT) methods: Koopmans’ theorem. The WF methods, especially post-Hartree-Fock with large bases sets, reach a satisfactory level of reproducibility on the calculation of ionization potential (IP) and orbital energies (), i.e., tend to fulfill the theorem, while pure DFT calculations provide poor .

A well-known failure in DFT calculation is the band gap underestimation in insulating materials and semiconductors, known as the "band-gap problem". The inclusion of the long-range correction (LC) in some DFT functionals gives the orbital energies close to the minus IPs, wherein our case it leads to an excellent result in the estimation of the 2-PY/2-HY relative stability. However, the same correction can be responsible for the detriment of the quality of the geometric parameters, which has impact on orbital and relative energy.

Our calculations with LC functionals shows the significant impact on bond lengths and angles in comparison to pure ones, especially for long-range parameter =0.47, wherein tend to Hartree-Fock geometry computation. In contrast to what we find in the literature for 2-PY/2-HY tautomerism, the relative energy is sensitive to geometry which in turn is susceptible to the theoretical method. Among the results of 127 functionals, our work extends on the LC-TPSSP86. The inclusion of the long-range parameter =0.04 gives excellent ge-

ometric parameters and the smaller root-mean-square errors on rotational constants in the comparison between pure DFT, MP2 and QCISD methods.

Our recipe for molecular stability prediction: The results of the theoretical method should rely in the 1) experimental/theoretical comparison of the geometric constants, 2) the smaller $K_{teo} = \text{vIP} + \text{HOMO}$ and 3) HOMO verified by experimental vertical ionization potential, from available measurements of the system and/or similar structures. The optimal long-range parameters, if necessary, can be found through the three steps we suggest. In the classic tautomeric case, the estimation of the relative stability by LC-TPSSP86 with $\alpha = 0.26$ to $\alpha = 0.47$ on good geometries, i.e., $\alpha = 0.04$, yields excellent agreement with experiments. Despite the computation with $\alpha = 0.47$ does not satisfy the steps 2 and 3, the E cancels the total energy error.

Solvent effects are described in excellent agreement with experiments and the calculations opens the way for the possibility to tuner the tautomeric equilibrium through directing groups. Besides the reproduction of the experimental data on 2-PY/2-HY case, our computations also show excellent concordance on relative stability assess in gas-phase of the formamide, 2-quinolinone, 2-pyrazinone, 2-quinoxalinone and 4-pyrimidinone at their respective temperatures. The analogous description for other compounds corroborates the reliability of our approach on the prediction of the molecular stability and its potential application: a guide to estimate molecular relative energy, to measure the confidence of the proposed reaction mechanisms by different theoretical methods, development of the molecular switches and computer-aided drug design.

Acknowledgement

The author is deeply grateful to Professor J.W.D. Carneiro, Ph.D candidate H.C. Silva Junior and Professor G.B. Ferreira for their useful suggestions and UFF Computational Chemistry Laboratory for the support.

References

- (1) Elguero, J.; Katritzky, A. R.; Denisko, O. Prototropic Tautomerism of Heterocycles: Heteroaromatic Tautomerism - General Overview and Methodology. *Advances in Heterocyclic Chemistry* **2000**, *76*, 1–84.
- (2) Raczyńska, E. D.; Kosińska, W.; Ośmiałowski, B.; Gawinecki, R. Tautomeric Equilibria in Relation to Pi-Electron Delocalization. **2005**,
- (3) Xu, H.; Gao, J.; Jiang, D. Stable, crystalline, porous, covalent organic frameworks as a platform for chiral organocatalysts. *Nature Chemistry* **2015**, *7*, 905–912.
- (4) Pospisil, P.; Ballmer, P.; Scapozza, L.; Folkers, G. Tautomerism in Computer-Aided Drug Design. *Journal of Receptors and Signal Transduction* **2003**, *23*, 361–371.
- (5) Martin, Y. C. Let's not forget tautomers. *Journal of computer-aided molecular design* **2009**, *23*, 693–704.
- (6) Wang, W.; Hellinga, H. W.; Beese, L. S. Structural evidence for the rare tautomer hypothesis of spontaneous mutagenesis. *Proceedings of the National Academy of Sciences of the United States of America* **2011**, *108*, 17644–8.
- (7) Florián, J.; Leszczyński, J. Spontaneous DNA Mutations Induced by Proton Transfer in the Guanine·Cytosine Base Pairs: An Energetic Perspective. *Journal of the American Chemical Society* **1996**, *118*, 3010–3017.
- (8) Liljeroth, P.; Repp, J.; Meyer, G. Current-Induced Hydrogen Tautomerization and Conductance Switching of Naphthalocyanine Molecules. *Science* **2007**, *317*, 1203–1206.
- (9) Zhang, J. L.; Zhong, J. Q.; Lin, J. D.; Hu, W. P.; Wu, K.; Xu, G. Q.; Wee, A. T. S.; Chen, W. Towards single molecule switches. *Chemical Society Reviews* **2015**, *44*, 2998–3022.

- (10) Piacenza, M.; Grimme, S. Systematic quantum chemical study of DNA-base tautomers. *Journal of Computational Chemistry* **2004**, *25*, 83–99.
- (11) Moore, C. M.; Dahl, E. W.; Szymczak, N. K. Beyond H₂: exploiting 2-hydroxypyridine as a design element from [Fe]-hydrogenase for energy-relevant catalysis. *Current Opinion in Chemical Biology* **2015**, *25*, 9–17.
- (12) Reetz, M. T. Combinatorial Transition-Metal Catalysis: Mixing Monodentate Ligands to Control Enantio-, Diastereo-, and Regioselectivity. *Angewandte Chemie International Edition* **2008**, *47*, 2556–2588.
- (13) Torres, M.; Gil, S.; Parra, M. New Synthetic Methods to 2-Pyridone Rings. *Current Organic Chemistry* **2005**, *9*, 1757–1779.
- (14) Baker, F.; Baly, E. C. C. CVI.—The relation between absorption spectra and chemical constitution. Part VII. Pyridine and some of its derivatives. *J. Chem. Soc., Trans.* **1907**, *91*, 1122–1132.
- (15) Meyer, H. Über reziproke sterische Beeinflussungen. *Monatshefte für Chemie* **1905**, *26*, 1303–1310.
- (16) Beak, P.; Fry, F. S.; Lee, J.; Steele, F. Equilibration studies. Protomeric equilibria of 2- and 4-hydroxypyridines, 2- and 4-hydroxypyrimidines, 2- and 4-mercaptopyridines, and structurally related compounds in the gas phase. *Journal of the American Chemical Society* **1976**, *98*, 171.
- (17) Nowak, M. J.; Lapinski, L.; Fulara, J.; Les, A.; Adamowicz, L. Matrix isolation IR spectroscopy of tautomeric systems and its theoretical interpretation: 2-hydroxypyridine/2(1H)-pyridinone. *The Journal of Physical Chemistry* **1992**, *96*, 1562–1569.

- (18) Brown, R. S.; Tse, A.; Vederas, J. C. Photoelectron-determined core binding energies and predicted gas-phase basicities for the 2-hydroxypyridine .dblew. 2-pyridone system. *Journal of the American Chemical Society* **1980**, *102*, 1174–1176.
- (19) Guimon, C.; Garrabe, G.; Pfister-Guillouzo, G. Spectroscopie photoelectronique a temperature variable equilibre prototropique des hydroxy-2 et mercapto-2 pyridines (1). *Tetrahedron Letters* **1979**, *20*, 2585–2588.
- (20) Held, A.; Champagne, B. B.; Pratt, D. W. Inertial axis reorientation in the S1 S0 electronic transition of 2-pyridone. A rotational Duschinsky effect. Structural and dynamical consequences. *The Journal of Chemical Physics* **1991**, *95*, 8732–8743.
- (21) Hatherley, L. D.; Brown, R. D.; Godfrey, P. D.; Pierlot, A. P.; Caminati, W.; Damiani, D.; Melandri, S.; Favero, L. B. Gas-phase tautomeric equilibrium of 2-pyridinone and 2-hydroxypyridine by microwave spectroscopy. *Journal of Physical Chemistry* **1993**, *97*, 46–51.
- (22) Aue, D. H.; Betowski, L. D.; Davidson, W. R.; Bowers, M. T.; Beak, P.; Lee, J. Gas-phase basicities of amides and imidates. Estimation of protomeric equilibrium constants by the basicity method in the gas phase. *Journal of the American Chemical Society* **1979**, *101*, 1361–1368.
- (23) Levin, E. S.; Rodionova, G. N. Tautomeric studies on lactams in the vapour state by infrared spectroscopy. *Dokl Akad. Nauk* **1965**, *164*, 910.
- (24) Smets, J.; Maes, G. Matrix-isolation FT-IR study on the protomeric tautomerism 2-hydroxypyridine2-pyridone. *Chemical Physics Letters* **1991**, *187*, 532–536.
- (25) Cook, M. J.; Katritzky, A. R.; Hepler, L. G.; Matsui, T. Heats of solution and tautomeric equilibrium constants. The 2-pyridone: 2-hydroxypyridine equilibrium in non-aqueous media. *Tetrahedron Letters* **1976**, *17*, 2685.

- (26) Mason, S. F. The tautomerism of N-heteroaromatic hydroxy-compounds. Part III. Ionisation constants. *Journal of the Chemical Society (Resumed)* **1958**, 674.
- (27) Schlegel, H. B.; Gund, P.; Fluder, E. M. Tautomerization of formamide, 2-pyridone, and 4-pyridone: an ab initio study. *Journal of the American Chemical Society* **1982**, *104*, 5347.
- (28) Fabian, W. M. F. Tautomeric equilibria of heterocyclic molecules. A test of the semiempirical AM1 and MNDO-PM3 methods. *Journal of Computational Chemistry* **1991**, *12*, 17–35.
- (29) Dkhissi, A.; Houben, L.; Smets, J.; Adamowicz, L.; Maes, G. Density functional theory and ab-initio computational study of the 2-hydroxypyridine/2-pyridone system: a comparison with FT-IR data from matrix isolation experiments. *Journal of Molecular Structure* **1999**, *484*, 215.
- (30) Gerega, A.; Lapinski, L.; Nowak, M. J.; Furmanchuk, A.; Leszczynski†, J. Systematic Effect of Benzo-Annellation on OxoHydroxy Tautomerism of Heterocyclic Compounds. Experimental Matrix-Isolation and Theoretical Study. *J. Phys. Chem. A* **2007**, *111*, 4934.
- (31) Maris, A.; Ottaviani, P.; Caminati, W. Pure rotational spectrum of 2-pyridone?water and quantum chemical calculations on the tautomeric equilibrium 2-pyridone...water/2-hydroxypyridine...water. *Chemical Physics Letters* **2002**, *360*, 155–160.
- (32) Wong, M. W.; Wiberg, K. B.; Frisch, M. J. Solvent effects. 3. Tautomeric equilibria of formamide and 2-pyridone in the gas phase and solution: an ab initio SCRF study. *Journal of the American Chemical Society* **1992**, *114*, 1645.
- (33) Kwiatkowski, J. S.; Leszczynski, J. Ab initio post-Hartree-Fock calculations of the 2-hydroxypyridine/2(1H)-pyridinone system: molecular structures, vibrational IR spectra

- and tautomeric stability. *Journal of Molecular Structure: THEOCHEM* **1994**, *312*, 201–213.
- (34) Sonnenberg, J. L.; Wong, K. F.; Voth, G. A.; Schlegel, H. B. Distributed Gaussian Valence Bond Surface Derived from Ab Initio Calculations. *Journal of Chemical Theory and Computation* **2009**, *5*, 949.
- (35) Fu, A.; Li, H.; Du, D.; Zhou, Z. Density Functional Study on the Reaction Mechanism of Proton Transfer in 2-Pyridone: Effect of Hydration and Self-Association. *J. Phys. Chem. A* **2005**, *109*, 1468.
- (36) Voth, G. A. *Computational approaches for studying enzyme mechanism. Part A*, pag 397, 1st ed.; Academic Press, 2016; Vol. 577.
- (37) Tsuneda, T.; Hirao, K. Long-range correction for density functional theory. *Wiley Interdisciplinary Reviews: Computational Molecular Science* **2014**, *4*, 375–390.
- (38) Iikura, H.; Tsuneda, T.; Yanai, T.; Hirao, K. A long-range correction scheme for generalized-gradient-approximation exchange functionals. *The Journal of Chemical Physics* **2001**, *115*, 3540–3544.
- (39) Forlani, L.; Cristoni, G.; Boga, C.; Todesco, P. E.; Vecchio, E. D.; Selva, S.; Monari, M. Reinvestigation of the tautomerism of some substituted 2-hydroxypyridines. *Arkivoc* **2002**, *2002*, 198.
- (40) Yang, H. W.; Craven, B. M.; IUCr, Charge Density Study of 2-Pyridone. *Acta Crystallographica Section B Structural Science* **1998**, *54*, 912.
- (41) Kvik, A.; Olovsson, I. No Title. *Arkiv fur Kemi* **1969**, *30*, 71.
- (42) Moreno, M.; Miller, W. H. On the tautomerization reaction 2-pyridone 2-hydroxypyridine: an ab initio study. *Chemical Physics Letters* **1990**, *171*, 475.

- (43) Moran, D.; Simmonett, A. C.; Leach, F. E.; Allen, W. D.; Schleyer, P. v. R.; Schaefer, H. F. Popular Theoretical Methods Predict Benzene and Arenes To Be Nonplanar. **2006**,
- (44) Papajak, E.; Zheng, J.; Xu, X.; Leverentz, H. R.; Truhlar, D. G. Perspectives on Basis Sets Beautiful: Seasonal Plantings of Diffuse Basis Functions. *Journal of Chemical Theory and Computation* **2011**, *7*, 3027–3034.
- (45) Cheeseman*, J. R.; Frisch, M. J.; And, F. J. D.; Stephens, P. J. Hartree-Fock and Density Functional Theory ab Initio Calculation of Optical Rotation Using GIAOs: Basis Set Dependence. **2000**,
- (46) P. J. Stephens, .; F. J. Devlin, .; ; J. R. Cheeseman, .; Frisch†, M. J. Calculation of Optical Rotation Using Density Functional Theory. **2001**,
- (47) Cook, M. J.; El-Abbady, S.; Katritzky, A. R.; Guimon, C.; Pfister-Guillouzo, G. Photoelectron spectra of hydroxy- and mercapto-pyridines and models of fixed structure. *Journal of the Chemical Society, Perkin Transactions 2* **1977**, *0*, 1652.
- (48) Tsuneda, T.; Song, J.-W.; Suzuki, S.; Hirao, K. On Koopmans’ theorem in density functional theory. *The Journal of Chemical Physics* **2010**, *133*, 174101.
- (49) Kar, R.; Song, J.-W.; Hirao, K. Long-range corrected functionals satisfy Koopmans’ theorem: Calculation of correlation and relaxation energies. *Journal of Computational Chemistry* **2013**, *34*, 958–964.
- (50) Lu, T.; Chen, F. Multiwfn: A multifunctional wavefunction analyzer. *Journal of Computational Chemistry* **2012**, *33*, 580–592.

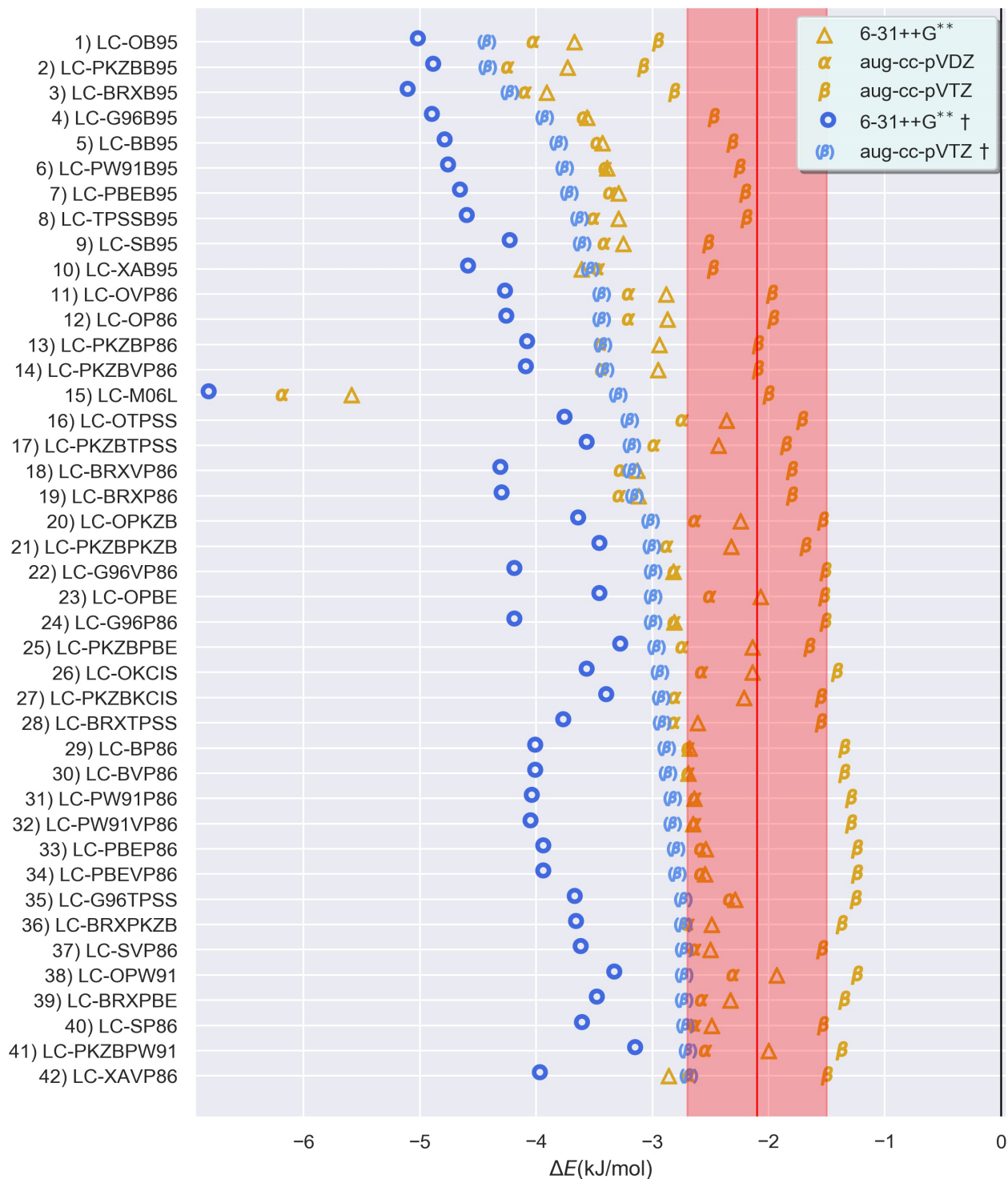


Figure 5: Our benchmark: Relative electronic energies, without zero point correction, of the 2-hydroxypyridine with respect to 2-pyridone in the gas-phase calculated by LC- functionals with $\omega = 0.47$, basis set in the legend. The dagger † means the calculation over geometric optimizations with long-range parameter $\omega = 0.04$. The correspondent experimental $\Delta E = -2.1(0.6)$ kJ/mol in red.¹⁷

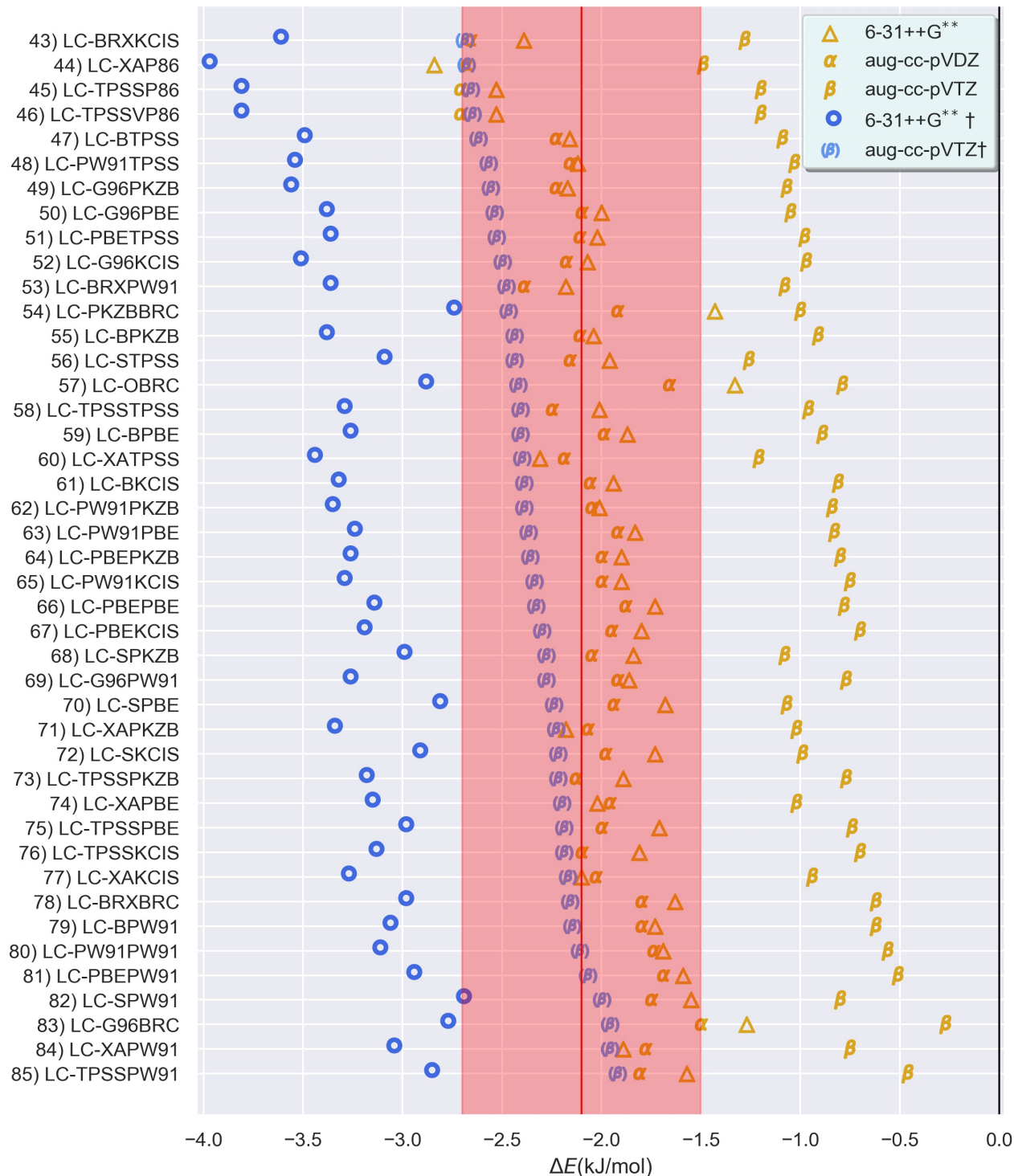


Figure 6: Our benchmark: Relative electronic energies, without zero point correction, of the 2-hydroxypyridine with respect to 2-pyridone in the gas-phase calculated by LC- functionals with $\omega = 0.47$, basis set in the legend. The dagger \dagger means the calculation over geometric optimizations with long-range parameter $\omega = 0.04$. The correspondent experimental $\Delta E = -2.1(0.6)$ kJ/mol in red.¹⁷

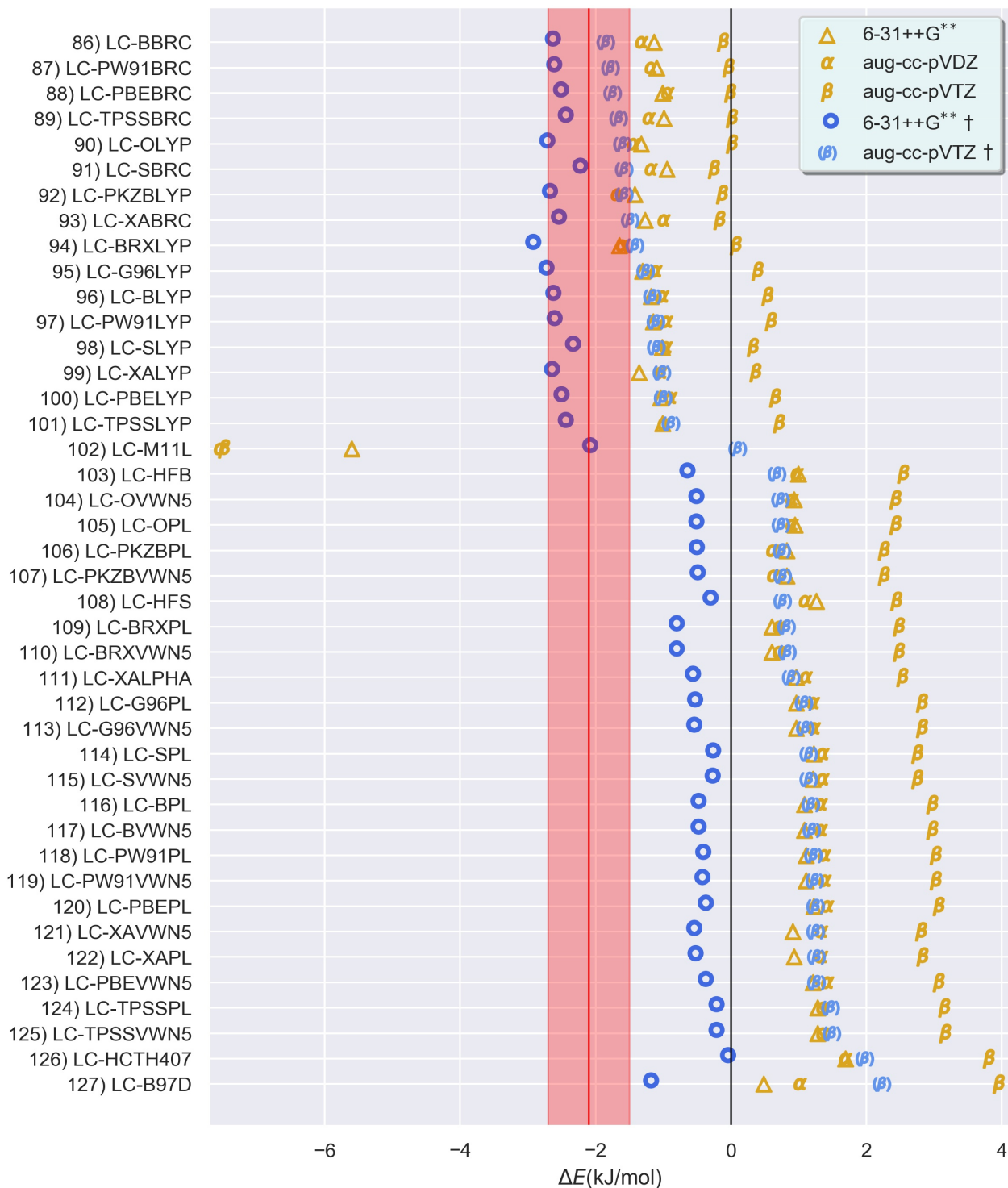


Figure 7: Our benchmark: Relative electronic energies, without zero point correction, of the 2-hydroxypyridine with respect to 2-pyridone in the gas-phase calculated by LC- functionals with $\omega = 0.47$, basis set in the legend. The dagger \dagger means the calculation over geometric optimizations with long-range parameter $\omega = 0.04$. The correspondent experimental $\Delta E = -2.1(0.6)$ kJ/mol in red.¹⁷